Journal of Systematics and Evolution 49 (3): 189–202 (2011) doi: 10.1111/j.1759-6831.2011.00124.x

Research Article

Efficiency of DNA barcodes for species delimitation: A case in *Pterygiella* Oliv. (Orobanchaceae)

[1,2]Li-Na DONG [3]Alexandra H. WORTLEY [1]Hong WANG* [1]De-Zhu LI [1]Lu LU

[1](*Key Laboratory of Biodiversity and Biogeography, and Plant Germplasm and Genomics Centre, Germplasm Bank of Wild Species, Kunming Institute of Botany, Chinese Academy of Sciences*, Kunming, Yunnan 650204, China)
[2](*Graduate School of Chinese Academy of Sciences*, Beijing 100039, China)
[3](*Royal Botanic Garden Edinburgh*, Edinburgh EH3 5LR, UK)

Abstract DNA barcoding is becoming an increasingly popular means to identify species. The obscure discrimination in the genus *Pterygiella* calls into question the re-assessment of the criterion for species delimitation. We collected 20 individuals, representing all five described species of this genus in its distributional range. The aim was to use three proposed barcode DNA regions (*rbcL*, *matK*, and ITS) to diagnose *Pterygiella* species, and examine which barcode is more suitable for discerning the congeneric and related species. The results showed that the core barcodes *matK* and *rbcL* were comparatively less effective. However, the ITS region, especially ITS-1 and ITS-2, successfully identified all species in the genus. Furthermore, the secondary structure of ITS-2 RNA, especially compensatory base changes, appears complementary to classical primary sequence analysis for DNA barcoding.

Key words compensatory base changes (CBCs), DNA barcode, ITS-2, non-monophyletic species, *Pterygiella* Oliv., secondary structure.

DNA barcoding is becoming an increasingly popular means of diagnosing species, based on the principle that sequence divergence is ordinarily much lower among individuals of a species than between closely related species. The approach could provide tools for the recognition of species limits and diversity, as an improvement on, or supplement to, traditional morphological taxonomy (Hebert et al., 2003; Hebert & Gregory, 2005; Packer et al., 2009). For example, in animals, short, standardized segments of the genome, such as cytochrome *c* oxidase I, have successfully been used as DNA barcodes to identify specimens rapidly and accurately even where taxonomic expertise is lacking (in birds, Hebert et al., 2004b; fish, Ward et al., 2005; and Lepidoptera, Hajibabaei et al., 2006). Furthermore, DNA barcoding has been shown to uncover species-level paraphyly and polyphyly in morphologically cryptic groups, through sampling multiple individuals from each species (Hebert et al., 2004a; Janzen et al., 2005; Newmaster & Ragupathy, 2009). Uncovering the prevalence of non-monophyletic species could improve taxonomic studies and increase our understanding of regional and global species diversity (Bickford et al., 2006).

In contrast to the animal kingdom, several different loci of the plastid genome (*rbcL*, *matK*, *trnH-psbA*, *rpoC1*, and *rpoB* and combinations thereof) have been proposed as suitable barcodes in plants (Chase et al., 2007; Newmaster et al., 2008; CBOL plant working group, 2009; Hollingsworth et al., 2009; Liu et al., 2010; Ren et al., 2010). Due to the frequency of reticulate evolution, facilitated by hybridization and genome duplication, species non-monophyly is likely to be very common in plants (Rieseberg & Brouillet, 1994). As a consequence, single plastid-based DNA barcodes cannot be relied upon to distinguish species. This problem will not necessarily be resolved simply by adding additional plastid DNA sequence data (Fazekas et al., 2009). In contrast, nuclear-encoded DNA sequences may provide improved species resolution in plants, owing to their generally higher synonymous substitution rate (Hajibabaei et al., 2006) and greater robustness to problems caused by hybridization (Chase et al., 2005).

The internal transcribed spacer (ITS) regions of nuclear ribosomal DNA have already been proposed as barcoding regions (Kress et al., 2005). Recently, internal transcribed spacer 2 (ITS-2) has been recommended as a promising DNA barcode in plants (Chen et al., 2010).

Received: 9 November 2010 Accepted: 30 January 2011
* Author for correspondence. E-mail: wanghong@mail.kib.ac.cn; Tel.: 86-871-5223534; Fax: 86-871-5217791.

© 2011 Institute of Botany, Chinese Academy of Sciences

万方数据

In one study of Fabaceae, Gao et al. (2010) found that 60–97% of species could successfully be identified using this single potential DNA barcode region. However, the researchers in this study focussed primarily on assessing the validity of ITS-2 as a DNA barcode at family level, rather than intense geographical sampling of congeneric and sibling species. In addition, they did not include the conserved secondary structure of ITS-2, which can provide reliable sequence alignment and can be used as a direct source of measurable information (Billoud et al., 2000; Coleman, 2003, 2007, 2009; Schultz et al., 2005; Schultz & Wolf, 2009). Yao et al. (2010) noticed that the secondary structure of the ITS-2 region could provide useful information for species identification. However, a further aspect of ITS-2 secondary structure, compensatory base changes (CBCs) – in which both nucleotides at a paired structural position are substituted while retaining their paired nucleotide bond – can also be used successfully to verify the taxonomy of closely related species (Müller et al., 2007; Ruhl et al., 2010). The characteristics of the secondary structure and CBCs of ITS-2 have needed further study for species delimitation in plant.

In this case study, we selected the three loci *matK*, *rbcL*, and ITS for the identification of species within *Pterygiella* Oliv. This genus was chosen for two reasons. First, *Pterygiella* is endemic to the eastern Himalaya–Hengduan Mountains region of China, whose very rich temperate flora (Wu, 1988) makes it one of the world's biodiversity hotspots. Second, species boundary and phylogenetic problems posed by the genus remain unresolved. *Pterygiella* is hemiparasitic and considered by most authors to comprise five species: *P. nigrescens* Oliv., *P. duclouxii* Franch., *P. cylindrica* Tsoong, *P. suffruticosa* D.Y. Hong, and *P. bartschioides* Hand.-Mazz. (e.g. Hong et al., 1998). Morphologically, *P. nigrescens* can be distinguished from the rest of the genus by its glandular-pubescent stem. *P. duclouxii* is morphologically similar to *P. nigrescens*, but can be distinguished by its wider distribution and glabrous to sparsely eglandular-hairy stem. According to Li (1950), *P. duclouxii* comprises two distinct varieties based on pubescence, leaf morphology, and distribution. *P. cylindrica* is identified by its terete stem and trinerved leaves, but can be differentiated from *P. suffruticosa* only by its herbaceous habit (Hong, 1996).

The final species, *P. bartschioides* is, according to Tao (1999), morphologically identical to *Xizangia serrata* D.Y. Hong, the sole species of *Xizangia* Hong, a genus endemic to southeastern Tibet. Wu (1999) also noticed the conspecific status of *X. serrata* and *P. bartschioides*. He maintained the generic rank of *Xizangia*, making the new combination *Xizangia bartschioides* (Hand.-Mazz.) C.Y. Wu & D.D. Tao. Based on morphological analysis, Hong (2001) stressed that *Xizangia* should be treated separately from *Pterygiella*. However, a subsequent study of pollen features failed to show any distinction between the two genera (Lu et al., 2007). Overall, the obscure discriminative morphological traits among these taxa call into question the accuracy of species delimitation within *Pterygiella*, as well as the generic status of *Xizangia*.

In the current study, we estimate the effectiveness of the potential chloroplast DNA barcodes *matK*, *rbcL*, and nrDNA ITS to differentiate species within *Pterygiella–Xizangia*, and examine the utility of secondary structural characters and CBCs in ITS-2 for distinguishing species within the complex. We address the following issues: (i) are *matK* and *rbcL* appropriate to identify *Pterygiella* species? (ii) if not, how does the ITS region perform as an alternative locus for barcoding species in the genus? and (iii) how effective is the ITS-2 secondary structure as a supplementary tool for distinguishing species?

1 Material and methods

1.1 Sampling and sequencing

Samples were obtained from 20 individuals of *Pterygiella*, including all five species [*P. bartschioides* was treated as *X. bartschioides* following the treatment of Wu (1999) and Hong (2001)] (Table 1). *Pterygiella duclouxii* was sampled with high geographical coverage including both potential varieties according to Li (1950). At least two individuals were sampled and sequenced for each species. Three outgroups were also sequenced for phylogenetic analyses: *Phtheirospermum*, considered to have a close relationship to *Pterygiella* (Li, 2002); *Rhinanthus*; and *Melampyrum* (S. Mathews, The Arnold Arboretum, Harvard University, Cambridge, pers. comm.).

Total DNA was isolated from silica gel-dried leaves following a modified CTAB protocol (Doyle & Doyle, 1987). The ITS region (including ITS-1, 5.8S, and ITS-2) was amplified using the primers ITS4 (5′-TCC TCC GCT TAT TGA TAT GC-3′) and ITS5 (5′-GGA AGG AGA AGT CGT AAC AAG G-3′) (White et al., 1990), the *matK* gene with primers IR (5′-ACC CAG TCC ATC TGG AAA TCT TGG TTC-3′) and 3F (5′-CGT ACA GTA CTT TTG TGT TTA CGA G-3′) (Kim, unpubl. data), and *rbcL* with primers IF (5′-ATG TCA CCA CAA ACA GAA AC-3′) and 724R (5′-TCG CAT GTA CCT GCA GTA GC-3′) (Fay et al., 1997). Polymerase chain reaction (PCR)

© 2011 Institute of Botany, Chinese Academy of Sciences

万方数据

Table 1 Voucher information and GenBank accession numbers for species examined in this study

Taxon	Locality	Latitude/longitude	Accession code	Voucher specimen	Herbarium code	*matK*	*rbcL*	ITS
Pterygiella cylindrica Tsoong	Muli, Sichuan, China	28°45′N/100°45′E	CML1	Dong LN, CML1	KUN	JF746407	JF746425	JF746385
P. cylindrica Tsoong	Muli, Sichuan, China	28°45′N/100°45′E	CML6	Dong LN, CML6	KUN	JF746409	JF746427	JF746387
P. cylindrica Tsoong	Muli, Sichuan, China	28°45′N/100°45′E	CML13	Dong LN, CML13	KUN	JF746408	JF746426	JF746386
P. duclouxii Franch.	Dali, Yunnan, China	25°69′N/100°17′E	DDL11	Dong LN, DL11	KUN	JF746410	JF746428	JF746388
P. duclouxii Franch.	Eryuan, Yunnan, China	26°15′N/99°91′E	DEY2	Dong LN, EY2	KUN	JF746412	JF746430	JF746390
P. duclouxii Franch.	Eryuan, Yunnan, China	26°15′N/99°91′E	DEY14	Dong LN, EY14	KUN	JF746411	JF746429	JF746389
P. duclouxii Franch.	Jiangchuan, Yunnan, China	24°48′N/102°86′E	DJC10	Dong LN, JC10	KUN	JF746413	JF746431	JF746384; JF746391
P. duclouxii Franch.	Muli, Sichuan, China	28°25′N/100°55′E	DML4	Dong LN, ML4	KUN	JF746415	JF746435	JF746395
P. duclouxii Franch.	Muli, Sichuan, China	28°25′N/100°55′E	DML15	Dong LN, ML15	KUN	–	JF746434	JF746394
P. duclouxii Franch.	Lijiang, Yunnan, China	26°89′N/100°23′E	DLJ5	Zhang S, LJ5	KUN	JF746414	JF746433	JF746393
P. duclouxii Franch.	Lijiang, Yunnan, China	26°89′N/100°23′E	DLJ10	Zhang S, LJ10	KUN	–	JF746432	JF746392
P. duclouxii Franch.	Xichang, Sichuan, China	27°89′N/102°26′E	DXC12	Yu WB, XC12	KUN	JF746416	JF746436	JF746396
P. nigrescens Oliv.	Nansha, Yunnan, China	23°22′N/102°83′E	NNS1	Dong LN, NS1	KUN	JF746417	JF746437	JF746397
P. nigrescens Oliv.	Nansha, Yunnan, China	23°22′N/102°83′E	NNS15	Dong LN, NS15	KUN	JF746418	JF746438	JF746398
P. suffruticosa D.Y. Hong	Shiping, Yunnan, China	23°71′N/102°49′E	SSP35	Dong LN, SP35	KUN	JF746421	JF746441	JF746401
P. suffruticosa D.Y. Hong	Shiping, Yunnan, China	23°71′N/102°49′E	SSP36	Dong LN, SP36	KUN	JF746422	JF746442	JF746402
P. suffruticosa D.Y. Hong	Muli, Sichuan, China	28°37′N/100°63′E	SML10	Dong LN, SML10	KUN	JF746419	JF746439	JF746399
P. suffruticosa D.Y. Hong	Muli, Sichuan, China	28°37′N/100°63′E	SML11	Dong LN, SML11	KUN	JF746420	JF746440	JF746400
Phtheirospermum tenuisectum Bureau & Franchet	Lijiang, Yunnan, China	–	–	Lu L, LJ377	KUN	–	–	JF746383
Melampyrum cartiense Fritsch	–	–	–	Krajsek s.n.	LJU	–	–	GU445314
M. klebelsbergianum Soó	Wuding, Yunnan, China	25°37′N/102°05′E		Dong LN, WD1	KUN	–	–	GU445315
Rhinanthus alectorolophus (Scop.) Pollich	–	–	–	Nyffler s.n.	GH	–	–	GU445318
R. freynii Fiori	–	–	–	Bennett 88	GH	–	–	GU445319
Xizangia bartschioides (Hand.-Mazz.) C.Y. Wu & D.D. Tao	Fugong, Yunnan, China	27°78′N/98°65′E	BGS3–2	Dong LN, GS3–2	KUN	JF746423	JF746443	JF746403; JF746404
X. bartschioides (Hand.-Mazz.) C.Y. Wu & D.D. Tao	Fugong, Yunnan, China	27°78′N/98°65′E	BGS6–8	Dong LN, GS6–8	KUN	JF746424	JF746444	JF746405; JF746406

–, no data.

© 2011 Institute of Botany, Chinese Academy of Sciences

万方数据

amplifications and procedures were carried out using standard methods (Dieffenbach & Dveksler, 2003). For specimens where initial sequencing failed, PCR products of ITS were ligated and transformed using a pEASY-T3 vector (TransGen Biotech, Beijing, China). Five to 10 clones were screened in each case; three of each were finally sequenced. Sequencing reactions were carried out with an ABI3100 automated sequencer (Applied Biosystems, Foster City, CA, USA).

1.2 Assessing homology of ITS sequences

The existence of paralogues, recombinants, and pseudogenes may cause problems with data from the ITS region, so these should be resolved through careful analysis (Buckler et al., 1997; Mayol & Rosselló, 2001; Bailey et al., 2003; Feliner & Rosselló, 2007). Thus, the following steps were taken to assess ITS sequences in the studied taxa. Dimethylsulfoxide was added to each reaction to enhance the diversity of amplifications (Buckler et al., 1997). Primers NNC 18S10 and C26A (Wen & Zimmer, 1996) were amplified and sequenced to compare with the sequenced results for ITS-4 and ITS-5 in several individuals. The nucleotide compositions of ITS-1, 5.8S, and ITS-2 were analysed separately using MEGA version 4.1 (Tamura et al., 2007). Secondary structures of 5.8S were generated using the DINAMelt server (http://dinamelt.bioinfo.rpi.edu/quikfold.php) as default values to estimate their minimum free energy. Each ITS sequence obtained was assessed according to the guidelines of Feliner & Rosselló (2007), and only reliable sequences were used for further study.

1.3 Inferring secondary structure of ITS-2 RNA

The ITS-2 RNA sequences were delimited using hidden Markov models (Keller et al., 2009) on the ITS-2 database web server (http://its2.bioapps.biozentrum.uni-wuerzburg.de/cgi-bin/index.pl). There are many approaches for predicting RNA secondary structure, including the Cocke–Younger–Kasami (CYK) algorithm for calculating minimum free energy in Mfold and RNAfold (Mathews et al., 1999; Zuker, 2003), and stochastic context-free grammars (Dowell & Eddy, 2004). Recently, a potentially more accurate measure of RNA secondary structure, the γ-centroid estimator, has been developed (Sato et al., 2009). Therefore, we inferred the secondary structures of ITS-2 rRNA using the CentroidFold online server in this study (http://www.ncrna.org/centroidfold). 4SALE (Seibel et al., 2006) was used for synchronous sequence and secondary structure alignment, editing, and depiction. The CBCAnalyzer (Wolf et al., 2005) was used to generate a CBC matrix (of uncorrected p-distances) and a simplified phylogram using the BIONJ algorithm.

1.4 Genetic analysis and species identification

Sequences of *matK*, *rbcL*, ITS-1, and 5.8S were aligned using the MUSCLE online server (http://www.ebi.ac.uk/Tools/muscle/index.html), and the final alignment was adjusted manually. Gaps were coded using the software GapCoder (Young & Healy, 2003). Pairwise K2P (Kimura 2-parameter) distances of *matK*, *rbcL*, *matK* + *rbcL*, ITS, ITS-1, 5.8S, and ITS-2 were calculated in MEGA version 4.1 (Tamura et al., 2007) to evaluate intraspecific and interspecific divergence in *Pterygiella*. The neighbor-joining (NJ) tree of K2P distances was created to provide a graphical representation of the divergence among species. We analysed two datasets: Dataset 1 used species delimitations for *Pterygiella* according to the *Flora of China* (Hong et al., 1998); Dataset 2 delimited species according to the molecular and morphological analysis in this study.

1.5 Phylogenetic analysis

We focused on the ITS-2 region of ITS for phylogenetic analysis, because the 5.8S region was found to have few parsimony-informative sites, and the ITS-1 region to have a higher transition rate than ITS-2. The ITS-2 regions were synchronous sequence and secondary structure aligned using 4SALE software (Seibel et al., 2006). Gaps were coded using GapCoder (Young & Healy, 2003). Phylogenetic trees were obtained under maximum parsimony (MP) and model-based (Bayesian) optimality criteria analyses. Parsimony analyses used heuristic searches using a branch-and-bound algorithm, with 1000 random taxon addition replicates in PAUP* 4.0b10 (Swofford, 2002). Node support was assessed by bootstrap (BS) resampling, with a branch-and-bound search algorithm and 1000 pseudoreplicates.

The optimal substitution model for the ITS-2 dataset was determined using the Akaike Information Criterion executed in the program MrModeltest (Posada & Crandall, 1998). Bayesian analyses were executed in MrBayes 3.1.2 (Ronquist & Huelsenbeck, 2003). The analyses were initiated with random trees and run for 1.0×10^5generations until the standard deviation of split frequencies was less than 0.01. The convergence between runs was assessed using the online application AWTY (Wilgenbusch et al., 2004; http://king2.scs.fsu.edu/CEBProjects/awty/awty_start.php). Posterior probability (PP) was used to estimate robustness.

© 2011 Institute of Botany, Chinese Academy of Sciences

万方数据

Table 2 Summary of polymerase chain reaction amplification results, sequencing success, and variability for *matK*, *rbcL*, internal transcribed spacer (ITS)-1, 5.8S and ITS-2. Intraspecific and interspecific distances were calculated based on the studied taxa

	matK	*rbcL*	*matK* + *rbcL*	ITS (all)	ITS-1	5.8S	ITS-2	CBCs
Aligned length (bp)	784	641	1425	627	231	161	235	–
Indel (length)	1 (6)	0	1 (6)	12 (1.2)	2 (1.2)	1 (1)	9 (1)	–
GC content	34.0%	43.3%	38.3%	58.3%	60.4%	55.4%	58.4%	–
No. parsimony information/variable sites	15/19	7/7	22/26	113/126	51/60	2/4	68/74	–
Species identified†	20%	20%	20%	20%	20%	20%	20%	20%
Species identified‡	33.3%	0%	0%	100%	100%	0%	100%	100%
Mean intraspecific variation (range)†	0.0006 (0.0000–0.0020)	0.0000	0.0000	0.0068 (0.0000–0.0190)	0.0102 (0.0000–0.0230)	0.0006 (0.0000–0.0030)	0.0078 (0.0000–0.0280)	0.4266 (0.0000–2.1330)
Minimum interspecific divergence (range)†	0.000 (0.000–0.018)	0.000 (0.000–0.011)	0.000 (0.000–0.011)	0.002 (0.002–0.176)	0.004 (0.004–0.205)	0.000 (0.000–0.020)	0.002 (0.002–0.279)	0.000 (0.000–8.750)
Mean intraspecific variation (range)‡	0.00075 (0.00000–0.00200)	0.00000	0.00000 (0.00000–0.00100)	0.00550 (0.00200–0.01200)	0.00930 (0.00100–0.02300)	0.00075 (0.00000–0.00300)	0.00500 (0.00200–0.00800)	0.06680 (0.00000–0.26700)
Minimum interspecific divergence (range)‡	0.001 (0.001–0.020)	0.000 (0.000–0.011)	0.000 (0.000–0.011)	0.032 (0.032–0.178)	0.040 (0.040–0.210)	0.000 (0.000–0.020)	0.046 (0.046–0.277)	3.611 (3.611–8.607)

†Statistics based on traditional classification according to the *Flora of China* (Hong et al., 1998; Dataset 1). ‡Statistics based on ITS-2 phylogenetic analysis presented in this study (Dataset 2).

2 Results

2.1 Evaluation of core and supplementary DNA barcodes

We obtained 18 *matK* sequences, 20 *rbcL* sequences, and 20 ITS sequences from the five species sampled. The total number of new sequences generated in this study was 58 (see Table 1). The minimum amplification rate using universal primers was 72% (found with *matK*). The PCR products were sequenced successfully for most accessions, but ITS sequencing failed in several cases due to polynucleotide tracts (particularly polyG/C) and hybrid peaks. Although the ITS region requires cloned PCR products for successful sequencing, it can be amplified and sequenced using universal primers, often even from herbarium collections.

For *matK*, the aligned sequence matrix was 784bp in length, including a 6bp indel in *P. duclouxii* DJC10. The matrix included 15 parsimony-informative sites and 19 variable sites. The *rbcL* matrix was 641bp in length (no indels) with seven parsimony-informative sites and seven variable sites. The aligned sequence matrix of ITS was 627bp in length, including 12 indels, with 113 parsimony-informative sites and 126 variable sites. Within ITS, ITS-1 and ITS-2 provided a greater number of informative and variable sites than the 5.8S region (Table 2).

Analysis showed that *matK*, *rbcL*, and nuclear ribosomal (nr)ITS failed to discriminate species by comparing inter- and intra-species divergence within the genus *Pterygiella* as DNA barcodes except for *Xizangia*, when *Pterygiella* was classified according to the *Flora of China* (Dataset 1). However, species were delimited according to a phylogenetic analysis of ITS-2 sequences (Dataset 2), ITS region, specifically ITS-1 and ITS-2 and a CBC matrix, was able to successfully identify all clades. By contrast, *matK* recognized only one clade (33.3%), whereas *rbcL*, *matK* + *rbcL*, and 5.8S still failed to identify any clades (Figs.1, 2).

2.2 Assessing homology of ITS sequences

Most taxa were successfully sequenced and identified using dimethylsulfoxide-enhanced reactions and different primers. The two exceptions, *P. duclouxii* DEY14 and *P. suffruticosa* SSP35 failed to be sequenced directly due to polynucleotide tracts, but were both sequenced successfully after cloning. *Pterygiella duclouxii* DJC10 exhibited two different sequences: *P. duclouxii* DJC10-clone 1 and *P. duclouxii* DJC10-clone 5, with 1.3% divergences. Divergence was concentrated in the ITS-1 and ITS-2 regions in these two sequences, but there was no difference in 5.8S region. In *X. bartschioides*, two sequences were discovered in both *X.*

© 2011 Institute of Botany, Chinese Academy of Sciences

万方数据

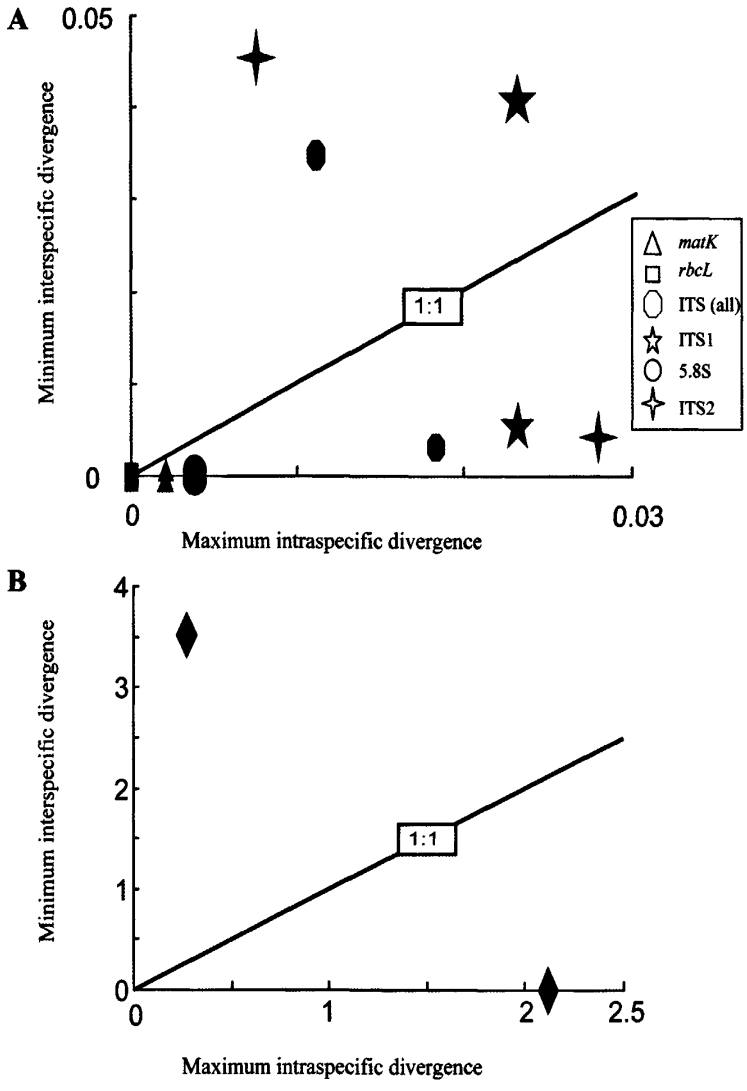

Fig. 1. Graphs showing presence or absence of sequence divergence necessary for successful barcoding. **A**, Sequence divergence in *matK*, *rbcL*, internal transcribed spacer (ITS; all), ITS-1, 5.8S, and ITS-2 in *Pterygiella*. **B**, Distance divergence for compensatory base changes across the same species in *Pterygiella*. Gray data points, Dataset 1 (*Flora of China* species delimitations); black data points, Dataset 2 (species delimited according to phylogenetic analysis in this study). Note that the scales in the two graphs differ.

bartschioides GS6–8 and *X. bartschioides* GS3–2. The variation was concentrated in the ITS-1 region; one transition (C→T) was found in the 5.8S region of *X. bartschioides* GS6–8-clone 1.

The characteristics of the ITS regions (ITS-1, 5.8S and ITS-2) are shown in Table 2. ITS-1 was slightly longer than ITS-2. The G+C content of the two spacer regions was approximately the same (60.4% for ITS-1 and 58.4% for ITS-2). Transitions (12) occurred at higher frequencies than transversions (five) in ITS-1, but transitions (four) appeared at lower frequencies than transversions (seven) in ITS-2. ITS-2 provided twice as many variable and informative sites as ITS-1. The 5.8S region was 161bp in length and contained one indel. Single nucleotide variations were discovered in *X. bartschioides* and *P. duclouxii* (sample DDL11). The minimum free energy was found to be constant throughout *Pterygiella*, but different and variable (−19.21Kcal/mol to −18.82Kcal/mol) in *Xizangia* (see Table 3).

2.3 Secondary structure of ITS-2 RNA

The ITS-2 secondary structures were found to have free energy values ranging from −77.20 Kcal/mol in *P. cylindrica* to −90.30Kcal/mol in *X. bartschioides*.

© 2011 Institute of Botany, Chinese Academy of Sciences

万方数据

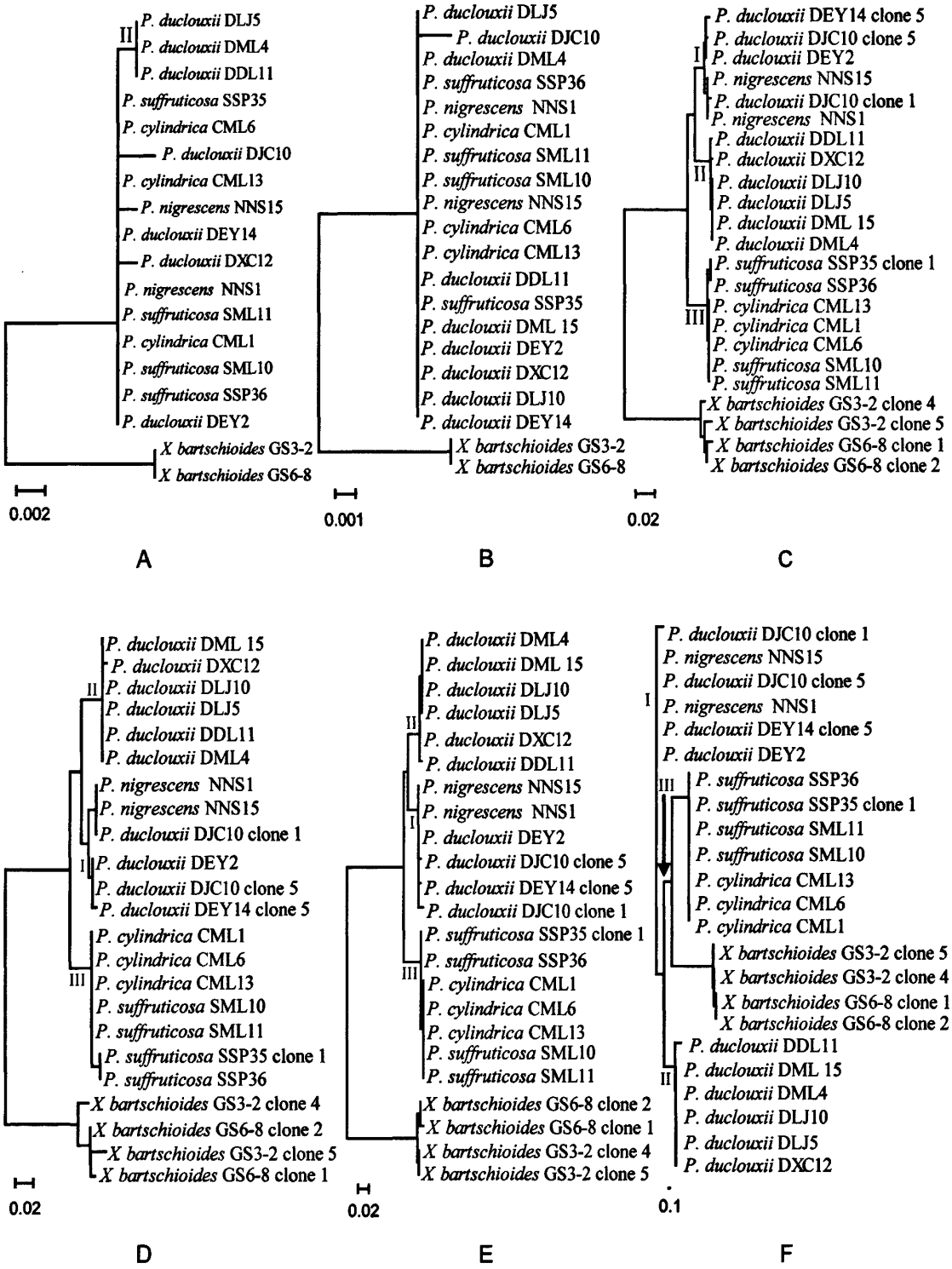

Fig. 2. Neighbor-joining trees produced from pairwise Kimura 2-parameter distances using MEGA 4.1 and profile neighbor joining tree obtained from compensatory base change (CBC) data using the CBCAnalyzer. **A,** *matK* matrix. **B,** *matK* + *rbcL* matrix. **C,** internal transcribed spacer (ITS) matrix. **D,** ITS-1 matrix. **E,** ITS-2 matrix. **F,** ITS-2 CBC matrix.

© 2011 Institute of Botany, Chinese Academy of Sciences

万方数据

Table 3 Statistics for the secondary structure of internal transcribed spacer (ITS)-2 proposed in this study

Taxon	Accession code	ITS-2					5.8S	
		G-U pairs	Helix length (bp)				ΔG (Kcal/mol)	ΔG (Kcal/mol)
			I	II	III	IV		
Pterygiella cylindrica	CML1	12	16	11	32	8	−77.20	−19.81
P. cylindrica	CML6	12	16	11	32	8	−77.20	−19.81
P. cylindrica	CML13	12	16	11	32	8	−77.20	−19.81
P. duclouxii	DDL11	12	18	11	31	8	−75.50	−19.81
P. duclouxii	DEY2	7	18	11	28	8	−87.70	−19.81
P. duclouxii	DEY14-clone5	7	18	11	28	8	−87.50	−19.81
P. duclouxii	DJC10-clone1	8	18	11	28	8	−89.90	−19.81
P. duclouxii	DJC10-clone5	7	18	11	28	8	−87.70	−19.81
P. duclouxii	DLJ5	10	17	11	31	8	−76.90	−19.81
P. duclouxii	DLJ10	10	17	11	31	8	−76.90	−19.81
P. duclouxii	DML4	10	17	11	31	8	−76.90	−19.81
P. duclouxii	DML15	10	17	11	31	8	−76.90	−19.81
P. duclouxii	DXC12	10	17	11	31	8	−77.50	−19.81
P. nigrescens	NNS1	7	18	11	28	8	−87.70	−19.81
P. nigrescens	NNS15	7	18	11	28	8	−87.70	−19.81
P. suffruticosa	SML10	11	16	11	32	8	−77.20	−19.81
P. suffruticosa	SML11	11	16	11	32	8	−77.20	−19.81
P. suffruticosa	SP35-clone1	11	17	11	32	8	−79.10	−19.81
P. suffruticosa	SSP36	11	17	11	32	8	−79.10	−19.81
Xizangia bartschioides	GS3–2-clone4	8	14	11	31	7	−80.10	−19.21
X. bartschioides	GS3–2-clone5	8	14	11	31	7	−80.10	−19.21
X. bartschioides	GS6–8-clone1	8	18	11	31	7	−90.30	−18.82
X. bartschioides	GS6–8-clone2	8	18	11	31	7	−90.30	−19.21

The structures displayed some universal features: four helices, a pyrimidine–pyrimidine bulge on helix II, and a UGGU sequence conserved on the 5′ side of helix III (Fig. 3). The two shorter helices (II and IV) were comparatively conservative (especially helix II), whereas the longer helices I and III showed higher variability. The proportion of G-U pairs in the helices was generally low (see Table 3).

We identified four distinct types of ITS-2 secondary structure, distinguished by morphometric characters of helices III and IV (Table 3; Fig. 3). Type I (Fig. 3:A) is identified by having 28 base pairs in helix III, and was found in the samples *P. duclouxii* DEY2, DEY14-clone 5, DJC10-clone 5, DJC10-clone 1, and DMZ1, and *P. nigrescens* NNS1 and NNS15. Type II (Fig. 3:B) can be recognised by having 31 base pairs in helix III, and was found in *P. duclouxii* DLJ5, DLJ10, DML4, DML15, and DXC12. Type III (Fig. 3:C) has 32 base pairs in helix III, and was found in *P. cylindrica* CML1, CML6, and CML13 and *P. suffruticosa* SML10, SML11, SSP35-clone 1, and SSP36. Type IV (Fig. 3:D) was distinct from the other three secondary structures in having 7 base pairs in the conserved helix IV; this structure was seen in *X. bartschioides* GS3–2-clone 4, GS3–2-clone 5, GS6–8-clone 1, and GS6–8-clone 2.

In comparisons between *Pterygiella* and *Xizangia*, CBCs were observed in helices I, III, and IV (Fig. 3, indicated by boxes). However, CBCs were not found in *P. duclouxii*, *P. nigrescens*, *P. cylindrica*, or *P. suffruticosa*. The CBC matrix divided *Pterygiella* into three clades (I, II, and III) with a further clade containing all *Xizangia* samples based on the NJ tree (Fig. 2:F). The three groups of *Pterygiella* identified by the NJ tree were supported by the secondary structure analysis: Group I comprises the taxa sharing Type I secondary structure; Group II those sharing Type II; and Group III those with Type III.

2.4 Phylogenetic analysis

The total length of the ITS-2 sequences after alignment of the 28 sampled taxa (including outgroups) was 297bp, with 39 indels and 123 parsimony-informative sites (41.4%). The single most parsimonious tree recovered had a length of 216 steps (consistency index = 0.884; retention index = 0.949; Fig. 4). The model selected was TVM+I by the Akaike Information Criterion implemented in MrModeltest. Phylogenies resulting from Bayesian analysis (not shown) were congruent in overall topology with those resulting from the parsimony analysis.

Phtheirospermum tenuisectum Bureau & Franchet was well supported as sister to the genus *Pterygiella* (100% BS, 1.00 PP). The separation of *Xizangia* from *Pterygiella* plus *Phtheirospermum* was well supported in both MP and Bayesian analyses (100% BS, 1.00 PP). Within *Pterygiella*, three major clades were resolved and well supported in both MP and Bayesian analyses (Fig. 4). Clade I comprised *P. duclouxii* DEY2,

© 2011 Institute of Botany, Chinese Academy of Sciences

万方数据

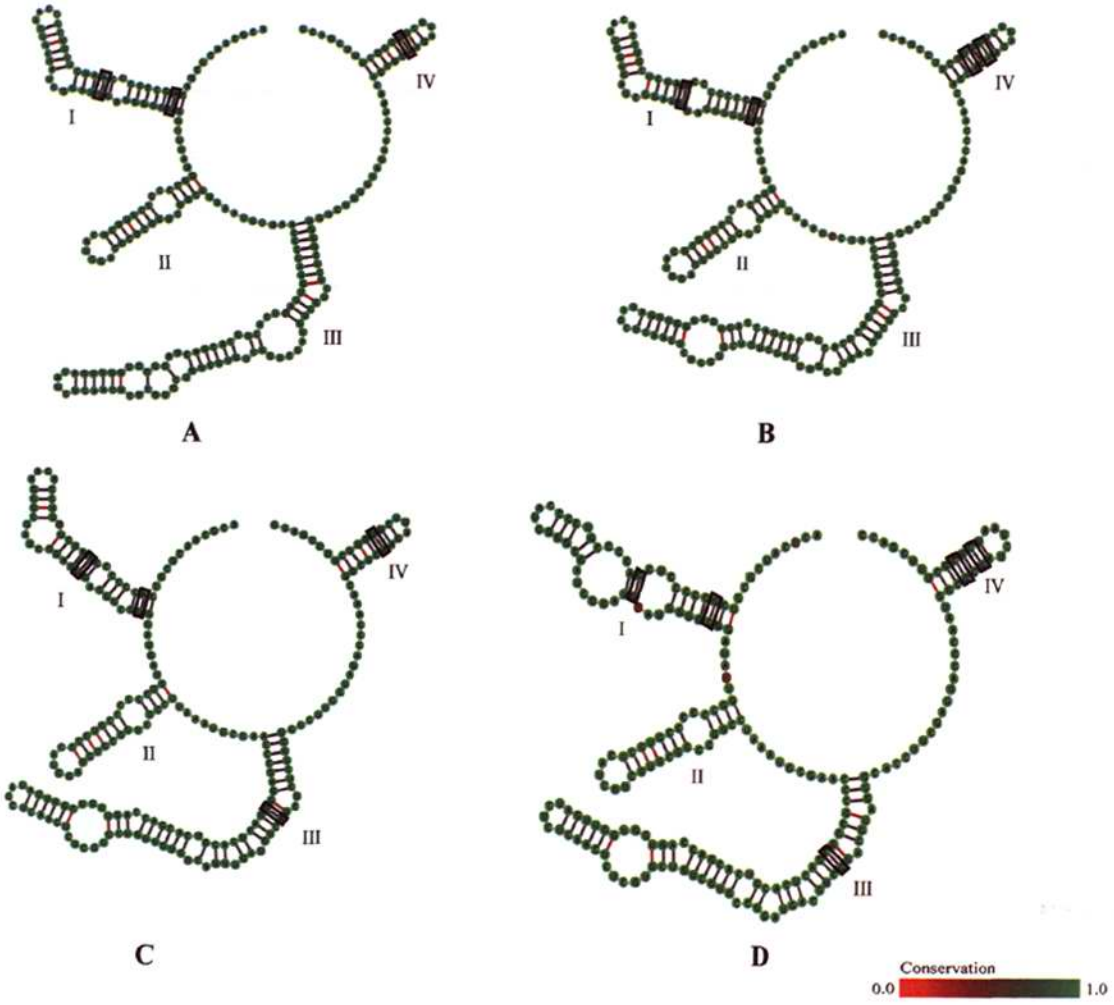

Fig. 3. Conservative secondary structure models for internal transcribed spacer-2 RNA, showing presence of compensatory base changes (indicated by boxes). **A**, Type I; **B**, Type II; **C**, Type III; **D**, Type IV. G:C and A:U base pairs are shown by dark gray lines, G:U pairs by red lines.

DEY14-clone 5, DJC10-clone 1 and DJC10-clone 5, and both *P. nigrescens* samples (97% BS, 1.00 PP). This clade was mainly distributed in southeastern Yunnan. Clade II comprises the remaining *P. duclouxii* samples: DDL11, DLJ5, DLJ10, DML4, DML15, and DXC12 (91% BS, 1.00 PP), distributed mainly in northwestern Yunnan and southern Sichuan. Clade III contained all sampled *P. cylindrica* and *P. suffruticosa* individuals (100% BS, 1.00 PP).

3 Discussion

We studied three potential DNA barcode regions (*matK*, *rbcL*, and nrITS) for species delimitation and discrimination in the *Pterygiella*. The chloroplast DNA barcode loci *matK*, *rbcL*, and *matK* + *rbcL* showed very low levels of discriminating power and were insufficient to discriminate taxa at species level in both Datasets 1 and 2 (*trnH-psbA* was also found to lack discriminating power; data not shown). In contrast, nrDNA ITS, particularly ITS-1 and ITS-2, effectively discriminated all species in the genus when circumscribed *Pterygiella* according to a phylogenetic and morphological analysis (Dataset 2).

Furthermore, the ITS-2 region provided useful information, as well as variability of primary sequence, in terms of molecular morphometrics of secondary structure and CBCs. These features of ITS-2 could provide powerful new information as a supplement to traditional barcode methodologies in taxonomic studies and species identification.

© 2011 Institute of Botany, Chinese Academy of Sciences

万方数据

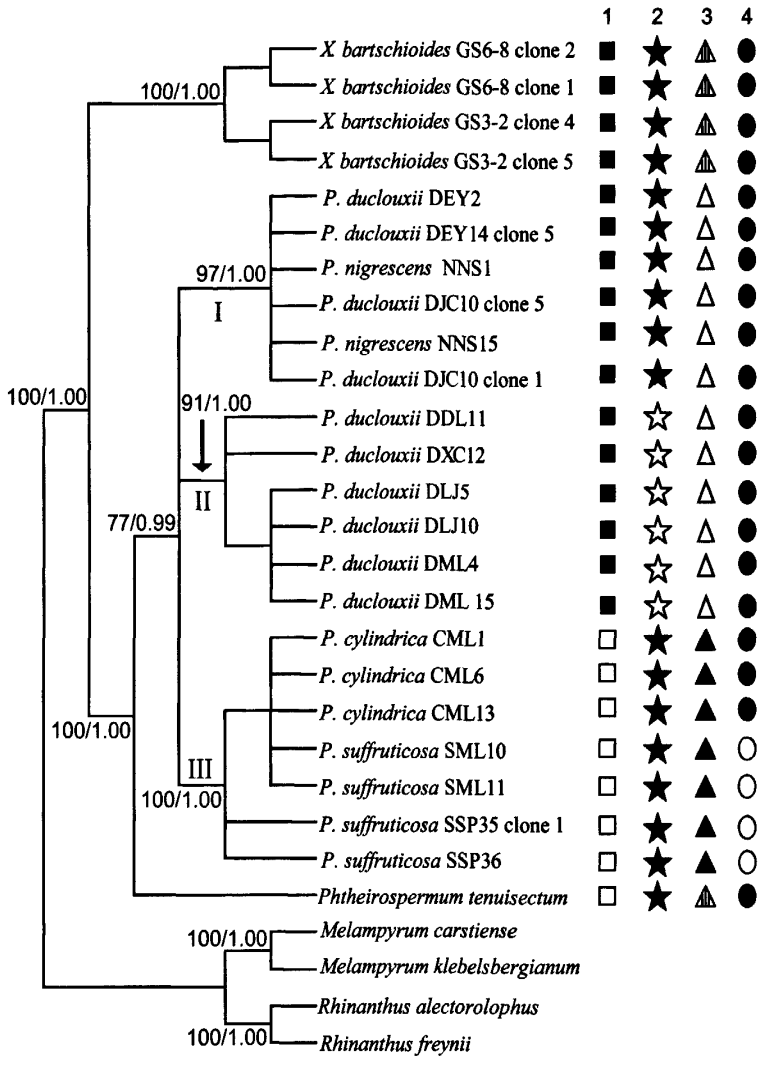

Fig. 4. Single most parsimonious tree inferred from nuclear internal transcribed spacer-2 DNA sequences. Numbers above branches indicate bootstrap percentage/posterior probability. Symbols to the right of the tree indicate character state distributions. 1, Stem: white square, quadrangular; black square, terete. 2, Indumentum: white pentagram, glandular; black pentagram, eglandular. 3, Veins: white triangle, uninerved; black triangle, trinerved; hatched triangle, multinerved. 4, Habit: white circle, shrubby; black circle, herb.

3.1 Species delimitation within *Pterygiella*

The classification of *Pterygiella* in *Flora of China* (Hong et al., 1998; Dataset 1) was found not to be based on monophyly, which resulted in failures in species identification using the core barcodes, *matK* and *rbcL*, and nrITS within the genus. Although these barcode regions showed less discrimination power in the genus *Pterygiella*, *Xizangia* was identified first in all conditions (Table 2; Figs. 1, 2). Furthermore, the phylogenetic analysis showed that *Xizangia* was separated from *Pterygiella*. Thus, we supported the elevation of *Xizangia* to generic status (Wu, 1999; Hong, 2001).

Based on a phylogenetic analysis of ITS-2 sequences, *P. duclouxii* was found to be non-monophyletic as currently circumscribed (Fig. 4). Possible explanations for the non-monophyletic species include imperfect analysis of morphological characters in previous taxonomies, interspecific hybridization, and incomplete lineage sorting (Funk & Omland, 2003). In this case, problematic morphology-based taxonomy is the most consistent explanation. Based on molecular and morphological analysis, *P. duclouxii* should be divided into two species or subspecies (Clades I and II), and that *P. nigrescens* should be included in one of these *P. duclouxii*

© 2011 Institute of Botany, Chinese Academy of Sciences

万方数据

taxa (Clade I), with which it shares eglandular hairs on the stem (Fig. 4).

The two species in Clade III, *P. suffruticosa* and *P. cylindrica*, display strong similarities in terms of both ITS-2 primary sequences and molecular morphometrics of ITS-2 RNA secondary structure (Table 3, Fig. 3). The level of inter- and intra-species variation in these two taxa does not support their distinction as species (Fig. 2). Morphologically, *P. suffruticosa* and *P. cylindrica* share homologous characters and are mainly distinguished on the basis of habit, a plastic character. We therefore consider *P. suffruticosa* should be treated as a variety of *P. cylindrica*.

When species within *Pterygiella* were redefined according to the phylogenetic analysis of ITS-2, not only did ITS-2 itself succeed as a DNA barcode, but the core barcode region *matK* also performed slightly better at species diagnosis, recognizing most taxa in Clade II. Furthermore, ITS-1 and a CBC matrix also supported the re-delimited classification of *Pterygiella*. These results support the assertion that ITS-2 can be used as a first approximation to delimit taxa for which variation within species makes it difficult to discern subtle signals from morphological noise (Packer et al., 2009).

3.2 Identifying multiple copies of ITS

It is notable that multiple copies of ITS were found in *P. duclouxii* DJC10 and *Xizangia*. Possible explanations for multiple copies include intraspecific polymorphisms, PCR or sequencing artefacts, non-concerted evolution among rDNA arrays, hybridization, and pseudogenes (Baldwin et al., 1995; Álvarez & Wendel, 2003).

In *Xizangia*, the pairwise K2P distances between copies of ITS were 0.5% in *X. bartschioides* GS6–8 and 1.3% in *X. bartschioides* GS3–2, which are lower than the intra-species divergence (1.4%) in *Xizangia*. Within the ITS region, although the primary sequences showed different levels of variation, the secondary structure was conserved across all copies. In the 5.8S region, a single transition (C→T) caused a slight decrease in minimum free energy without influencing the secondary structures in *X. bartschioides* GS6–8-clone 1. In the ITS-1 region, sequence divergence between copies was mainly located in this region and was attributable to irregular point mutations; the secondary structure has a conserved AAGGAA motif in all copies, which may help to ensure correct processing (Liu & Schardl, 1994). In the ITS-2 region, the primary sequence and secondary structure were found to be stable. Thus, all different copies have functional sequences, and the most likely explanation was PCR or sequencing artefacts for these multiple copies of *Xizangia* individuals.

In *P. duclouxii* DJC10, the secondary structures of ITS contained all the conserved motifs in both copies, which excluded the possibility that these were pseudogenes or paralogues (Feliner & Rosselló, 2007). The variations were mainly focused on the ITS-2 region and can be divided into two possible types according to the minimum free energy of the secondary structure of ITS-2 (Buckler et al., 1997). Moreover, the sequence divergence found between ITS copies in *P. duclouxii* DJC10 (1.8%) far exceeded the mean intra-species divergence in the genus (0.5%). Furthermore, based on analysis of ITS, *P. duclouxii* DJC10-clone 5 was closer to *P. duclouxii* DEY, and *P. duclouxii* DJC10-clone 1 was closer to *P. nigrescens*. In terms of distribution, *P. duclouxii* DJC was located between *P. duclouxii* DEY and *P. nigrescens*. Therefore, the polymorphism in *P. duclouxii* DJC10 could be explained as hybrid diploids, which needs further study. On the whole, in neither case do the multiple copies of ITS-2 sequences present a problem to their treatment as a barcode marker.

3.3 Secondary structure of ITS-2 RNA

Compared to ITS-1 and the 5.8S region, ITS-2 primary sequences showed greatest divergence, but the secondary structures showed greatest conservation. Thus, the characteristics of ITS-2 secondary structure contain more potential information than those of ITS-1 and 5.8S, and may be complementary to classical primary sequence analysis for distinguishing species. In the present study, the morphometrics of secondary structure provided information to identify species in agreement with primary sequence analysis. Moreover, although the CBCs of ITS-2 structure showed less inter- and intra-specific variation than ITS-2 sequences, they were also applicable to delimiting closely related species (Ruhl et al., 2010). Furthermore, using the ITS-2 database and analysis tools freely available online (e.g. http://its2.bioapps.biozentrum.uni-wuerzburg.de/cgi-bin/index.pl?about), the secondary structure of ITS-2 could provide a way to distinguish species. Nevertheless, further study is needed to gain a better understanding of the effectiveness of ITS-2 sequences and structure within larger sample sizes.

3.4 Feasibility of ITS-2 as a supplementary barcode region

The main criteria that should be considered when evaluating genetic loci for potential use in plant DNA barcoding are: (i) significant species-level genetic

© 2011 Institute of Botany, Chinese Academy of Sciences

万方数据

variability and divergence; (ii) an appropriately short sequence length to facilitate DNA extraction and amplification; and (iii) the presence of conserved flanking sites for developing universal primers (Kress et al., 2005). With relation to these criteria, the nrITS region has frequently been proposed as a potential nuclear barcode (e.g. Cowan et al., 2006; Liu et al., 2010; Ren et al., 2010). The effectiveness of ITS-2 sequences to identify species has also been demonstrated empirically (Ben-David et al., 2007; Chen et al., 2010; Gao et al., 2010). Furthermore, secondary structures of ITS-2 can provide effective information as a DNA barcode to identify species (Prasad et al., 2009; Yao et al., 2010).

However, the effectiveness of ITS has been questioned in the light of complex evolutionary patterns in the region. We consider that the region should not be ruled out before it has been tested using next generation sequencing technologies, for several reasons. First, the region can easily be amplified and sequenced using universal primers in the context of the nuclear genome, even in long-preserved specimens. Second, the conserved secondary structure of ITS-2 provides a tool to resolve the complex evolutionary patterns by assessment and screening of paralogues, pseudogenes, and sequencing artefacts (Feliner & Rosselló, 2007). Finally, analysis of sequence and secondary structure is simple and routine using current software (e.g. 4SALE and CBCAnalyzer) and the ITS-2 online database (http://its2.bioapps.biozentrum.uni-wuerzburg.de/cgi-bin/index.pl?about).

Although the present study considered only a small endemic genus, it nonetheless indicates that the use of ITS-2 secondary structures and CBCs should be expanded to provide a supplementary plant DNA barcode, at least in intractable taxa where routine DNA barcodes have been found problematic.

Acknowledgements The authors would like to thank the following people for their assistance: Sarah MATHEWS from Harvard University (Cambridge, MA, USA) for providing DNA extraction methods for the outgroup; Mei-Qing YANG for laboratory work; You-Jie ZHAO and Wen-Kai JIANG for their advice on inferring ITS-2 secondary structure; Jie LIU in data analysis; and Yu-Xiao ZHANG and Ram Chandra POUDEL for their comments on a first draft of this manuscript. This research was supported by the National Natural Science Foundation of China (Grant No. 30970201), and the Research Fund for the Large-scale Scientific Facilities of CAS (Grant No. 2009-LSF-GBOWS-01).

References

Álvarez I, Wendel JF. 2003. Ribosomal ITS sequences and plant phylogenetic inference. Molecular Phylogenetics and Evolution 29: 417–434.

Bailey CD, Carr TG, Harris SA, Hughes CE. 2003. Characterization of angiosperm nrDNA polymorphism, paralogy, and pseudogenes. Molecular Phylogenetics and Evolution 29: 435–455.

Baldwin BG, Sanderson MJ, Porter JM, Wojciechowski MF, Campbell CS, Donoghue MJ. 1995. The ITS region of nuclear ribosomal DNA: A valuable source of evidence on angiosperm phylogeny. Annals of the Missouri Botanical Garden 82: 247–277.

Ben-David T, Melamed S, Gerson U, Morin S. 2007. ITS2 sequences as barcodes for identifying and analyzing spider mites (Acari: Tetranychidae). Experimental and Applied Acarology 41: 169–181.

Bickford D, Lohman DJ, Sodhi NS, Ng PKL, Meier R, Winker K, Ingram KK, Das I. 2006. Cryptic species as a window on diversity and conservation. Trends in Ecology and Evolution 22: 148–155.

Billoud B, Guerrucci MA, Masselot M, Deutsch JS. 2000. Cirripede phylogeny using a novel approach: Molecular morphometrics. Molecular Biology and Evolution 17: 1435–1445.

Buckler ES, Ippolito A, Holtsford TP. 1997. The evolution of ribosomal DNA: Divergent paralogues and phylogenetic implications. Genetics 145: 821–832.

CBOL plant working group. 2009. A DNA barcode for land plants. Proceedings of the National Academy of Sciences USA 106: 12794–12797.

Chase MW, Salamin N, Wilkinson M, Dunwell JM, Kesanakurthi RP, Haidar N, Savolainen V. 2005. Land plants and DNA barcodes: Short-term and long-term goals. Philosophical Transactions of the Royal Society B: Biological Sciences 360: 1889–1895.

Chase MW, Cowan RS, Hollingsworth PM, van den Berg C, Madriñán S, Petersen G, Seberg O, Jørgsensen T, Cameron KM, Carine M, Pedersen N, Hedderson TAJ, Conrad F, Salazar GA, Richardson JE, Hollingsworth ML, Barraclough TG, Kelly L, Wilkinson M. 2007. A proposal for a standardised protocol to barcode all land plants. Taxon 56: 295–299.

Chen SL, Yao H, Han JP, Liu C, Song JY, Shi LC, Zhu YJ, Ma XY, Gao T, Pang XH, Luo K, Li Y, Li XW, Jia XC, Lin YL, Leon C. 2010. Validation of the ITS2 region as a novel DNA barcode for identifying medicinal plant species. PLoS One 5: e8613.

Coleman AW. 2003. ITS2 is a double-edged tool for eukaryote evolutionary comparisons. Trends in Genetics 19: 370–375.

Coleman AW. 2007. Pan-eukaryote ITS2 homologies revealed by RNA secondary structure. Nucleic Acids Research 35: 3322–3329.

Coleman AW. 2009. Is there a molecular key to the level of "biological species" in eukaryotes? A DNA guide. Molecular Phylogenetics and Evolution 50: 197–203.

Cowan RS, Chase MW, Kress WJ, Savolainen V. 2006. 300,000 species to identify: Problems, progress, and prospects in DNA barcoding of land plants. Taxon 55: 611–616.

© 2011 Institute of Botany, Chinese Academy of Sciences

万方数据

Dieffenbach CW, Dveksler GS. 2003. PCR primer. A laboratory manual, 2nd edition. New York: Cold Spring Harbor Laboratory Press.

Dowell RD, Eddy SR. 2004. Evaluation of several lightweight stochastic context-free grammars for RNA secondary structure prediction. BMC Bioinformatics 5: 71.

Doyle JJ, Doyle JL. 1987. A rapid DNA isolation procedure for small quantities of fresh leaf tissue. Phytochemical Bulletin 19: 11–15.

Fay MF, Swensen SM, Chase MW. 1997. Taxonomic affinities of *Medusagyne oppositifolia* (Medusagynaceae). Kew Bulletin 52: 111–120.

Fazekas AJ, Kesanakurti PR, Burgess KS, Percy DM, Graham SW, Barrett SCH, Newmaster SG, Hajibabaei M, Husband BC. 2009. Are plant species inherently harder to discriminate than animal species using DNA barcoding markers? Molecular Ecology Resources 9: 130–139.

Feliner GN, Rosselló JA. 2007. Better the devil you know? Guidelines for insightful utilization of nrDNA ITS in species-level evolutionary studies in plants. Molecular Phylogenetics and Evolution 44: 911–919.

Funk DJ, Omland KE. 2003. Species-level paraphyly and polyphyly: Frequency, causes, and consequences, with insights from animal mitochondrial DNA. Annual Review of Ecology, Evolution, and Systematics 34: 397–423.

Gao T, Yao H, Song JY, Liu C, Zhu YJ, Ma XY, Pang XH, Xu HX, Chen SL. 2010. Identification of medicinal plants in the family Fabaceae using a potential DNA barcode ITS2. Journal of Ethnopharmacology 130: 116–121.

Hajibabaei M, Janzen DH, Burns JM, Hallwachs W, Hebert PDN. 2006. DNA barcodes distinguish species of tropical Lepidoptera. Proceedings of the National Academy of Sciences USA 103: 968–971.

Hebert PDN, Gregory TR. 2005. The promise of DNA barcoding for taxonomy. Systematic Biology 54: 852–859.

Hebert PDN, Cywinska A, Ball SL, deWaard JR. 2003. Biological identifications through DNA barcodes. Proceedings of the Royal Society B: Biological Sciences 270: 313–321.

Hebert PDN, Penton EH, Burns JM, Janzen DH, Hallwachs W. 2004a. Ten species in one: DNA barcoding reveals cryptic species in the neotropical skipper butterfly *Astraptes fulgerator*. Proceedings of the National Academy of Sciences USA 101: 14812–14817.

Hebert PDN, Stoeckle MY, Zemlak TS, Francis CM. 2004b. Identification of birds through DNA barcodes. PLoS Biology 2: e312.

Hollingsworth ML, Clark A, Forrest LL, Richardson J, Pennington RT, Long DG, Cowan R, Chase MW, Gaudeul M, Hollingsworth P. 2009. Selecting barcoding loci for plants: Evaluation of seven candidate loci with species-level sampling in three divergent groups of land plants. Molecular Ecology Resources 9: 439–457.

Hong DY. 1996. Additional notes on the Scrophulariaceae of China. Novon 6: 372–374.

Hong DY. 2001. *Xizangia bartschioides* (Hand.-Mazz.) D.Y. Hong, a new combination in Scrophulariaceae. Acta Phytotaxonomica Sinica 39: 544–546.

Hong DY, Yang HB, Jin CL, Holmgren NH. 1998. Scrophulariaceae. In: Flora Reipublicae Popularis Sinicae. Beijing: Science Press. 18: 209–211.

Janzen DH, Hajibabaei M, Burns JM, Hallwachs W, Remigio E, Hebert PDN. 2005. Wedding biodiversity inventory of a large and complex Lepidoptera fauna with DNA barcoding. Philosophical Transactions of the Royal Society B: Biological Sciences 360: 1835–1845.

Keller A, Schleicher T, Schultz J, Müller T, Dandekar T, Wolf M. 2009. 5.8S-28S rRNA interaction and HMM-based ITS2 annotation. Gene 430: 50–57.

Kress WJ, Wurdack KJ, Zimmer EA, Weigt LA, Janzen DH. 2005. Use of DNA barcodes to identify flowering plants. Proceedings of the National Academy of Sciences USA 102: 8369–8374.

Li HL. 1950. Vicarism in the geography of the Scrophulariaceae in China. Taiwania 1: 141–153.

Li XW. 2002. Notes on some botanical names from China. Acta Botanica Yunnanica 24: 14–16.

Liu JS, Schardl CL. 1994. A conserved sequence in internal transcribed spacer 1 of plant nuclear rRNA genes. Plant Molecular Biology 26: 775–778.

Liu Y, Yan HF, Cao T, Ge XJ. 2010. Evaluation of 10 plant barcodes in Bryophyta (Mosses). Journal of Systematics and Evolution 48: 36–46.

Lu L, Wang H, Blackmore S, Li DZ, Dong LN. 2007. Pollen morphology of the tribe Rhinantheae (Orobanchaceae) and its systematic significances. Plant Systematics and Evolution 268: 177–198.

Mathews DH, Sabina J, Zuker M, Turner DH. 1999. Expanded sequence dependence of thermodynamic parameters improves prediction of RNA secondary structure. Journal of Molecular Biology 288: 911–940.

Mayol M, Rosselló JA. 2001. Why nuclear ribosomal DNA spacers (ITS) tell different stories in *Quercus*. Molecular Phylogenetics and Evolution 19: 167–176.

Müller T, Philippi N, Dandekar T, Schultz J, Wolf M. 2007. Distinguishing species. RNA 13: 1496–1472.

Newmaster SG, Ragupathy S. 2009. Testing plant barcoding in a sister species complex of pantropical *Acacia* (Mimosoideae, Fabaceae). Molecular Ecology Resources 9: 172–180.

Newmaster SG, Fazekas AJ, Steeves RAD, Janovec J. 2008. Testing candidate plant barcode regions in the Myristicaceae. Molecular Ecology Resources 8: 480–490.

Packer L, Gibbs J, Sheffield C, Hanner R. 2009. DNA barcoding and the mediocrity of morphology. Molecular Ecology Resources 9: 42–50.

Posada D, Crandall KA. 1998. ModelTest: Testing the model of DNA substitution. Bioinformatics 14: 817–818.

Prasad PK, Tandon V, Biswal DK, Goswami LM, Chatterjee A. 2009. Use of sequence motifs as barcodes and secondary structures of internal transcribed spacer 2 (ITS2, rDNA) for identification of the Indian liver fluke, *Fasciola* (Trematoda: Fasciolidae). Bioinformation 3: 314–320.

Ren BQ, Xiang XG, Chen ZD. 2010. Species identification of *Alnus* (Betulaceae) using nrDNA and cpDNA genetic markers. Molecular Ecology Resources 10: 594–605.

Rieseberg LH, Brouillet L. 1994. Are many plant species paraphyletic? Taxon 43: 21–32.

Ronquist F, Huelsenbeck JP. 2003. MrBayes 3: Bayesian phylogenetic inference under mixed models. Bioinformatics 19: 1572–1574.

© 2011 Institute of Botany, Chinese Academy of Sciences

万方数据

Ruhl MW, Wolf M, Jenkins TM. 2010. Compensatory base changes illuminate morphologically difficult taxonomy. Molecular Phylogenetics and Evolution 54: 664–669.

Sato K, Hamada M, Asai K, Mituyama T. 2009. CentroidFold: A web server for RNA secondary structure prediction. Nucleic Acids Research 37: W277–W280.

Schultz J, Wolf M. 2009. ITS2 sequence-structure analysis in phylogenetics: A how-to manual for molecular systematics. Molecular Phylogenetics and Evolution 52: 520–523.

Schultz J, Maisel S, Gerlach D, Müller T, Wolf M. 2005. A common core of secondary structure of the internal transcribed spacer 2 (ITS2) throughout the Eukaryota. RNA 11: 361–364.

Seibel PN, Müller T, Dandekar T, Schultz J, Wolf M. 2006. 4SALE – a tool for synchronous RNA sequence and secondary structure alignment and editing. BMC Bioinformatics 7: 498.

Swofford DL. 2002. PAUP*: Phylogenetic analysis using parsimony (*and other methods), version 4.0b10. Sunderland: Sinauer Associates.

Tamura K, Dudley J, Nei M, Kumar S. 2007. MEGA4: Molecular evolutionary genetics analysis (MEGA) software version 4.0. Molecular Biology and Evolution 24: 1596–1599.

Tao DD. 1999. The identity of the genus *Xizangia* Hong (Scrophulariaceae). Acta Phytotaxonomica Sinica 37: 281.

Ward RD, Zemlak TS, Innes BH, Last PR, Hebert PDN. 2005. DNA barcoding Australia's fish species. Philosophical Transactions of the Royal Society B: Biological Sciences 360: 1847–1857.

Wen J, Zimmer EA. 1996. Phylogeny and biogeography of *Panax* L. (the Ginseng genus, Araliaceae): inferences from ITS sequences of nuclear ribosomal DNA. Molecular Phylogenetics and Evolution 6: 167–177.

White TJ, Bruns T, Lees S, Taylor J. 1990. Amplification and direct sequencing of fungal ribosomal RNA genes for phylogenetics. In: Innis M, Gelfand D, Sninsky J, White T eds. PCR protocols: A guide to methods and applications. San Diego: Academic Press. 315–322.

Wilgenbusch JC, Warren DL, Swofford DL. 2004. AWTY: A system for graphical exploration of MCMC convergence in Bayesian phylogenetic inference [online]. Available from http://ceb.csit.fsu.edu/awty.

Wolf M, Friedrich J, Dandekar T, Müller T. 2005. CBCAnalyzer: Inferring phylogenies based on compensatory base changes in RNA secondary structures. In Silico Biology 5: 291–294.

Wu ZY. 1988. Hengduan mountain flora and her significance. Journal of Japanese Botany 63: 297–311.

Wu ZY. 1999. Two new combinations in Chinese Scrophulariaceae. Novon 9: 288.

Yao H, Song JY, Liu C, Luo K, Han JP, Li Y, Pang XH, Xu HX, Zhu YJ, Xiao PG, Chen SL. 2010. Use of ITS2 region as the universal DNA barcode for plants and animals. PLoS One 5: e13102.

Young ND, Healy J. 2003. GapCoder automates the use of indel characters in phylogenetic analysis. BMC Bioinformatics 4: 6.

Zuker M. 2003. Mfold web server for nucleic acid folding and hybridization prediction. Nucleic Acids Research 31: 3406–3415.

© 2011 Institute of Botany, Chinese Academy of Sciences

万方数据

万方数据 WANFANG DATA 文献链接

Efficiency of DNA barcodes for species delimitation: A case in Pterygiella Oliv.(Orobanchaceae)

作者： Li-Na DONG， Alexandra H. WORTLEY， Hong WANG， De-Zhu LI， Lu LU

作者单位： Li-Na DONG(Key Laboratory of Biodiversity and Biogeography, and Plant Germplasm and Genomics Centre, Germplasm Bank of Wild Species, Kunming Institute of Botany,Chinese Academy of Sciences, Kunming, Yunnan 650204, China; Graduate School of Chinese Academy of Science)， Alexandra H. WORTLEY(Royal Botanic Garden Edinburgh, Edinburgh EH3 5LR, UK)， Hong WANG,De-Zhu LI,Lu LU(Key Laboratory of Biodiversity and Biogeography, and Plant Germplasm and Genomics Centre, Germplasm Bank of Wild Species, Kunming Institute of Botany,Chinese Academy of Sciences, Kunming, Yunnan 650204, China)

刊名： 植物分类学报 ISTIC SCI PKU

英文刊名： JOURNAL OF SYSTEMATICS AND EVOLUTION

年，卷(期)： 2011,49(3)

本文链接：http://d.g.wanfangdata.com.cn/Periodical_zwflxb201103005.aspx